

Proton–induced deuteron breakup at GeV energies with forward emission of a fast proton pair ¹

V. Komarov ^{a,*}, S. Dymov ^{b,a}, A. Kacharava ^{c,d}, A. Kulikov ^a,
G. Macharashvili ^{a,d}, A. Petrus ^a, F. Rathmann ^b, H. Seyfarth ^b,
H. Ströher ^b, Yu. Uzikov ^{a,e}, S. Yaschenko ^{c,a}, B. Zalikhanov ^a,
M. Büscher ^b, W. Erven ^f, M. Hartmann ^b, A. Khoukaz ^g,
R. Koch ^b, V. Kurbatov ^a, N. Lang ^g, R. Maier ^b, S. Merzliakov ^a,
S. Mikirtychiants ^h, H. Müller ⁱ, M. Nioradze ^d, H. Ohm ^b,
D. Prasuhn ^b, R. Santo ^g, H. Paetz ^{gen}, Schieck ^j,
R. Schleichert ^b, H.J. Stein ^b, K. Watzlawik ^b, N. Zhuravlev ^a,
and K. Zvoll ^f

^a*Joint Institute for Nuclear Research, LNP, 141980 Dubna, Russia*

^b*Institut für Kernphysik, FZJ, 52425 Jülich, Germany*

^c*Phys. Inst. II, Universität Erlangen–Nürnberg, 91058 Erlangen, Germany*

^d*High Energy Physics Institute, Tbilisi State University, 380086 Tbilisi, Georgia*

^e*Kazakh National University, 480078 Almaty, Kazakhstan*

^f*Zentrallabor für Elektronik, FZJ, 52425 Jülich, Germany*

^g*Institut für Kernphysik, Universität Münster, 48149 Münster, Germany*

^h*St. Petersburg Nuclear Physics Institute, 188350 Gatchina, Russia*

ⁱ*Institut für Kern- und Hadronenphysik, FZR, 01474 Dresden, Germany*

^j*Institut für Kernphysik, Universität zu Köln, 50937 Köln, Germany*

Abstract

A study of the deuteron breakup reaction $pd \rightarrow (pp)n$ with forward emission of a fast proton pair with small excitation energy $E_{pp} < 3$ MeV has been performed using the ANKE spectrometer at COSY–Jülich. An exclusive measurement was carried out at six proton–beam energies $T_p = 0.6, 0.7, 0.8, 0.95, 1.35,$ and 1.9 GeV by reconstructing the momenta of the two protons. The differential cross section of the breakup reaction, averaged up to 8° over the cm polar angle of the total momentum of the pp pairs, has been obtained. Since the kinematics of this process is quite similar to that of backward elastic $pd \rightarrow dp$ scattering, the results are compared to calculations based on a theoretical model previously applied to the $pd \rightarrow dp$ process.

Key words: Deuteron breakup; Short–range nucleon–nucleon interaction

PACS: 13.75.Cs, 25.10.+s, 25.40-h.

1 Introduction

Backward elastic $pd \rightarrow dp$ scattering at energies of several hundred MeV is one of the simplest hadron–nucleus processes with high transferred momentum. It has been studied for more than 30 years both experimentally and

* Corresponding author: V. Komarov

Email address: v.komarov@fz-juelich.de (V. Komarov).

¹ This paper is dedicated to A. Petrus who was killed in a tragic accident on May 19, 2002.

theoretically with the aim of extracting information about the short-range structure of the NN interaction and the dynamics of high-momentum transfer in few-nucleon systems. Besides the one-nucleon-exchange (ONE) mechanism (Fig. 1), a number of concepts have been discussed in this context, e.g. the presence of nucleon resonances (N^*) inside the deuteron [1], the importance of virtual pions [2], and three-baryon resonances [3] (for a review see Ref. [4]). Only at low energies, where ONE dominates, are the data on differen-

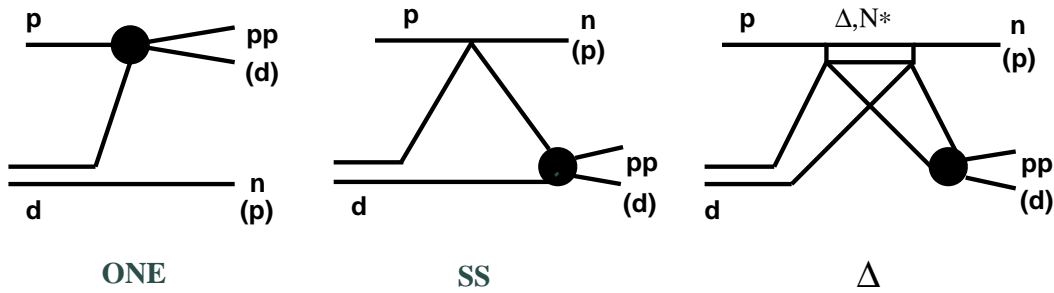


Fig. 1. Mechanisms included in the ONE+SS+ Δ model for the $pd \rightarrow (pp)n$ ($pd \rightarrow dp$) processes.

tial cross section, tensor analyzing power T_{20} , and spin transfer coefficient κ , reasonably well described [4-8]. At higher energies, where internal momenta above 0.3 GeV/c are probed in the deuteron, the dynamics becomes more complicated, because of a possible excitation of N^* and Δ resonances in the intermediate states. These effects are taken into account to some extent in the one-pion-exchange model, but when adding the ONE amplitude, the problem of double counting arises [2,9,10]. The excitation of the $\Delta(1232)$ resonance in the intermediate state (Δ mechanism) is explicitly included in a model [3,5], which also takes into account coherently ONE and single pN scattering (SS) in a consistent way (Fig. 1). This model, improved in Ref. [11] with respect to the Δ contribution through the analysis of $pp \rightarrow pn\pi^+$ data [12], describes the

gross features of the $pd \rightarrow dp$ spin-averaged differential cross section. After further refinement also the tensor analyzing power at beam energies below 0.5 GeV is qualitatively reproduced [5]. Above the region, where the $\Delta(1232)$ dominates, the role of intermediate excitations of heavier baryon resonances is expected to increase and this makes the theoretical interpretation of this process much more ambiguous.

In view of the above complications, it would be very important to study a similar pd process, where contributions from the N^* and Δ resonance excitation are suppressed. For that purpose, an appropriate reaction is the deuteron breakup

$$p + d \rightarrow (pp) + n$$

with emission of the two protons in forward direction ($\theta_{pp} \approx 0^\circ$) at low excitation energy $E_{pp} < 3$ MeV. With the neutron emitted backward, the kinematics of this reaction is quite close to that of pd backward elastic scattering. Therefore, the same mechanisms can be applied in the analysis of the process as well. According to the ONE+SS+ Δ model calculations [13,14], which implicitly include the pp final-state interaction (fsi), the pp pair is expected to be mainly in a 1S_0 state. Due to isospin invariance, the isovector nature of the pp pair leads to a suppression of the amplitude of the Δ mechanism by a factor three in comparison to the ONE amplitude for all partial waves of the pp system [13]. The same suppression factor also applies for a broad class of diagrams with isovector meson-nucleon rescattering in the intermediate state, including excitation of N^* resonances [15]. As a result, the contribution of the ONE mechanism, which is sensitive to the NN potential at short distances, becomes more pronounced than in $pd \rightarrow dp$ scattering. Furthermore, the node in the half-off-shell pp scattering amplitude in the 1S_0 state at an off-shell

momentum of about 0.4 GeV/c leads to a dip of the differential cross section of the deuteron breakup at 0.7–0.8 GeV beam energy [13,16]. At higher energies of 1–3 GeV, the cross section is dominated by the ONE mechanism and decreases rather smoothly.

Another attractive feature of the process is the simplicity of its phenomenological description, since at zero degrees it requires only two spin amplitudes. Therefore, a model-independent amplitude analysis becomes possible through the measurement of a few polarization observables. As a first step, we have measured the differential cross section at six beam energies in the interval 0.6–1.9 GeV, which covers the region of the dip predicted by the ONE+SS+ Δ model, thereby probing a wide range of high internal momenta of the NN system ($q_{NN} \sim 0.3$ –0.6 GeV/c).

2 Experiment

The experiment was performed at incident proton beam energies of 0.6, 0.7, 0.8, 0.95, 1.35, and 1.9 GeV with the spectrometer ANKE [17] at the internal beam of the COoler SYnchrotron COSY-Jülich [18]. In Fig. 2 those parts of the spectrometer are shown that are of concern for the present experiment. The protons stored in the COSY ring ($\sim 3 \cdot 10^{10}$) impinged on a deuterium cluster-jet target [19], which provided a target thickness of about $1.3 \cdot 10^{13}$ atoms/cm². The produced charged particles, after passing the magnetic field of the dipole D2, were registered by a set of three multiwire proportional chambers (MWPC) and a scintillation-counter hodoscope. Each wire chamber contains a horizontal and a vertical anode-wire plane (1 mm wire spacing), and two planes of inclined strips, that allowed us to obtain the re-

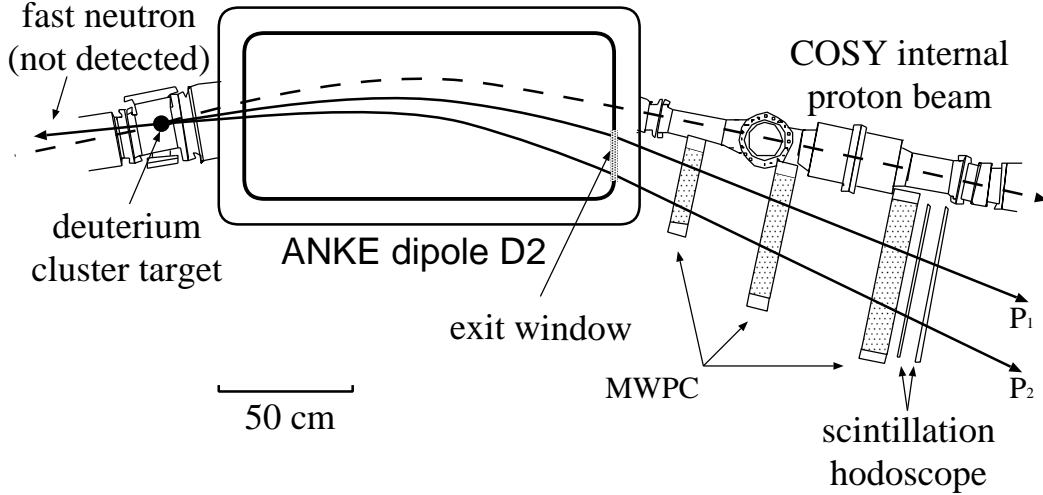


Fig. 2. Top view of the experimental setup with the forward detection system of the ANKE spectrometer.

quired resolution of $\approx 0.8\text{--}1.2\%$ (rms) in the momentum range $0.6\text{--}2.7\text{ GeV}/c$. The hodoscope consists of two layers, containing 8 and 9 vertically oriented scintillators (4 to 8 cm width, 1.5 to 2 cm thickness). It provided a trigger signal, an energy loss measurement, and allowed for the determination of the differences in arrival times for particle pairs hitting different counters. Off-line processing of the amplitude data permitted the measurement of the energy-loss with an accuracy of 10 to 20% (FWHM), and of the time-of-flight difference of events with two registered particles with a precision of 0.5 ns (rms). A separate measurement with a hydrogen target at beam energies of 0.5 and 2.65 GeV was carried out to calibrate the energy loss in the counters and the momentum scale via the processes $pp \rightarrow pp$, $pp \rightarrow d\pi^+$, and $pp \rightarrow pn\pi^+$.

The horizontal acceptance of the setup is shown in Fig. 3. The vertical acceptance corresponds to $\pm 3.5^\circ$. The trigger rate resulted mainly from elastically and quasi-elastically scattered protons, from protons associated with meson production and, at beam energies below 1 GeV, from deuterons produced in

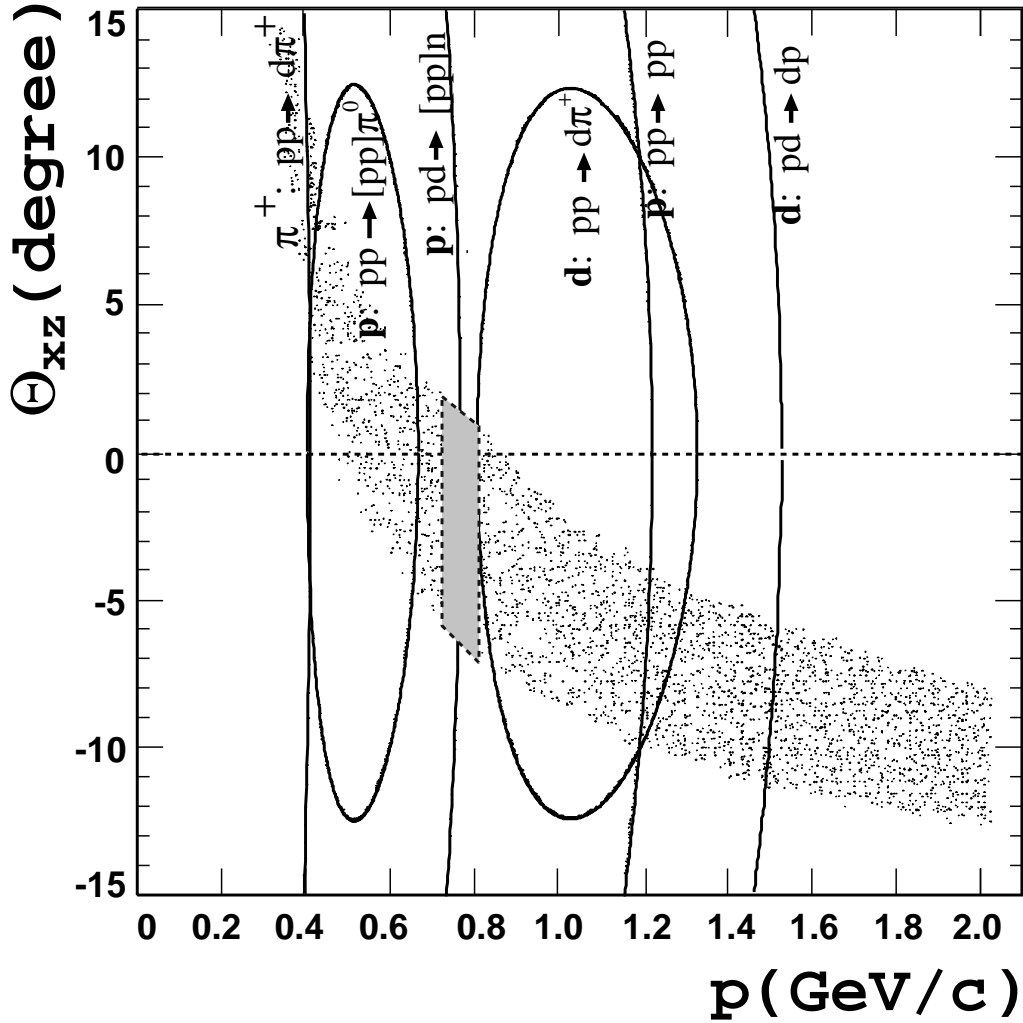


Fig. 3. Plot of the acceptance of the setup from a MC simulation showing polar angle versus momentum at 0.6 GeV beam energy. Θ_{xz} is the scattering angle of the emitted particle projected onto the median plane of the spectrometer. The curves show kinematical loci for π^+ , p, and d from the indicated processes. The symbol [pp] denotes pp pairs with zero excitation energy, while the grey area contains those of $E_{pp} < 3$ MeV.

the $pp \rightarrow d\pi^+$ reaction. Events with two registered particles contributed little to the total trigger rate and were selected off-line. Protons from the breakup process $pd \rightarrow ppn$ with an excitation energy $E_{pp} < 3$ MeV could be detected

with the experimental setup for laboratory polar angles between 0 and 7° at all energies.

Among those events with two registered particles, breakup events are identified by the determination of the missing-mass value, calculated under the assumption that these particles are protons. At all energies the missing-mass spectra reveal a well defined peak at the neutron mass with an rms value of about 20 MeV (Fig. 4). The peak is clearly separated from the one at 1.1–

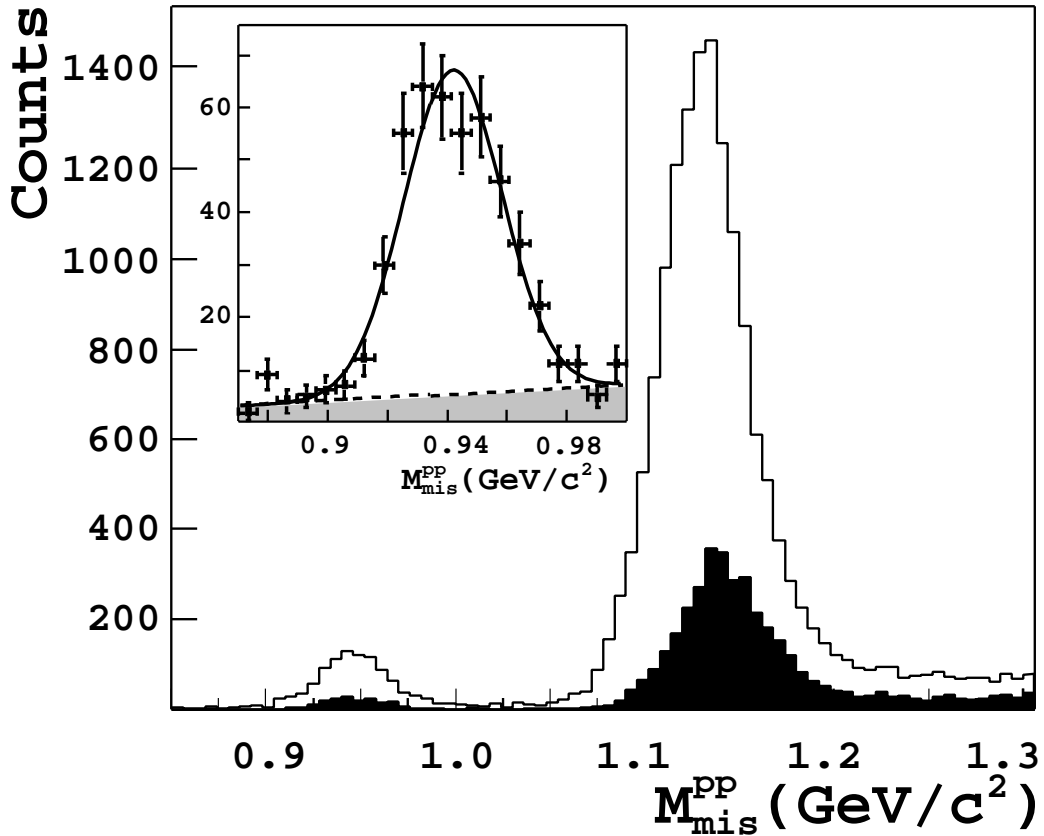


Fig. 4. Missing-mass distribution at $T_p = 0.8$ GeV of all identified proton pairs (unfilled histogram). The black histogram denotes identified pp pairs with excitation energy of less than 3 MeV. The inset shows the distribution near the neutron mass without particle identification for pairs with $E_{pp} < 3$ MeV. The background contribution is shown in grey.

1.2 GeV/c², caused by proton pairs from the $pd \rightarrow pp\pi^0n$ or $pd \rightarrow pp\pi^-p$ reactions. A direct identification of the particle type is possible for those events for which the two particles hit different counters in the hodoscope. These amount to about 60% of all events in the peak at the neutron mass. For $E_{pp} < 3$ MeV, the fraction varies from 60 to 22% for $T_p = 0.6$ to 1.9 GeV. The time-of-flight difference Δt measured in the hodoscope was compared to the difference $\Delta t(p_1, p_2)$ obtained from the reconstructed particle momenta p_1 and p_2 , again assuming that the two particles are protons. Applying a 2σ cut to the peak of the $\Delta t - \Delta t(p_1, p_2)$ distribution, proton pairs could be selected such that the contribution from other pairs was less than 1%. When both tracks hit the same counter, the energy loss distributions were analyzed and found to be in agreement with the assumption that both registered particles were protons. However, the energy loss cut was not used, since the proton separation from other particles was not quite perfect. In this case we relied on the fact that misidentified pairs ($p\pi^+$, $d\pi^+$, dp or ${}^3\text{H}\pi^+$) show up only at substantially higher missing mass values and therefore cannot contribute to the peak at the neutron mass. For background subtraction, the spectra in the vicinity of the neutron mass were fitted by the sum of a Gaussian and a straight line (see inset in Fig. 4). The number of proton pairs and the signal-to-background ratio $N_{\text{sig}}/N_{\text{bg}}$ were determined in a $\pm 2\sigma$ range around the neutron mass. The distribution of distances between hits by the proton pairs ($E_{pp} < 3$ MeV) in the MWPC's yields rms values of 4.9 and 3.3 cm, at 0.6 and 1.9 GeV beam energies, respectively. Therefore, a significant loss of pp pairs due to the two tracks being too close is expected to occur only below $E_{pp} = 0.2$ MeV. Since a resolution of 0.2 (0.3) MeV at $E_{pp} = 0.5$ (3) MeV was achieved, proton pairs with $E_{pp} < 3$ MeV could be reliably selected.

The integrated luminosity L^{int} was obtained by counting protons, elastically

and quasi-elastically scattered at small laboratory angles between 5 and 10°. It is not possible to distinguish these processes experimentally at ANKE, but the achieved momentum resolution makes possible a clean separation from the meson production continuum. The number of counts obtained was related to a simulation using the calculated small angle $pd \rightarrow pX$ cross section. The calculation takes into account the sum of elastic and inelastic terms in closure approximation of the Glauber–Franco theory [20], which includes the sum over the complete set of final pn states. In order to estimate the obtained accuracy, the cross sections, calculated for elastic and quasielastic pd scattering within the same framework, were compared with the experimental data of Refs. [21,22,23,24,25] and [26] respectively, in the appropriate energy and angle range. The resulting $\chi^2/n.d.f.=0.85$ (n.d.f.=64) and $\chi^2/n.d.f.=0.73$ (n.d.f.=8), respectively, yield a 7% uncertainty of the calculated cross sections. The total errors of the luminosities of Table 1 take into account this uncertainty and other systematic errors of 5%, resulting from a small variation of the derived luminosity with the polar angle, caused by the position–dependent efficiency of the MWPC.

3 Results and discussion

The data allowed us to deduce the three–fold differential cross sections $d^3\sigma/(d \cos \theta_{pp}^{\text{cm}} \cdot d\phi_{pp}^{\text{cm}} \cdot dE_{pp})$, where θ_{pp}^{cm} and ϕ_{pp}^{cm} are the polar and azimuthal cm angles of the total momentum of the pp pair, respectively. (The neutron emission angles correspond to $180^\circ - \theta_{pp}^{\text{cm}}$). Figure 5 shows the excitation energy distribution of the events for θ_{pp}^{cm} from 0 to 7° and ϕ_{pp}^{cm} from 0 to 360°, summed over the beam energies 0.6, 0.7, and 0.8 GeV. The shape of the spectrum is

well reproduced ($\chi^2/n.d.f.=0.99$) by the phase space distribution multiplied by the Migdal–Watson factor describing the 1S_0 fsi [27] including Coulomb effects. The event distribution over the angle between the relative momentum

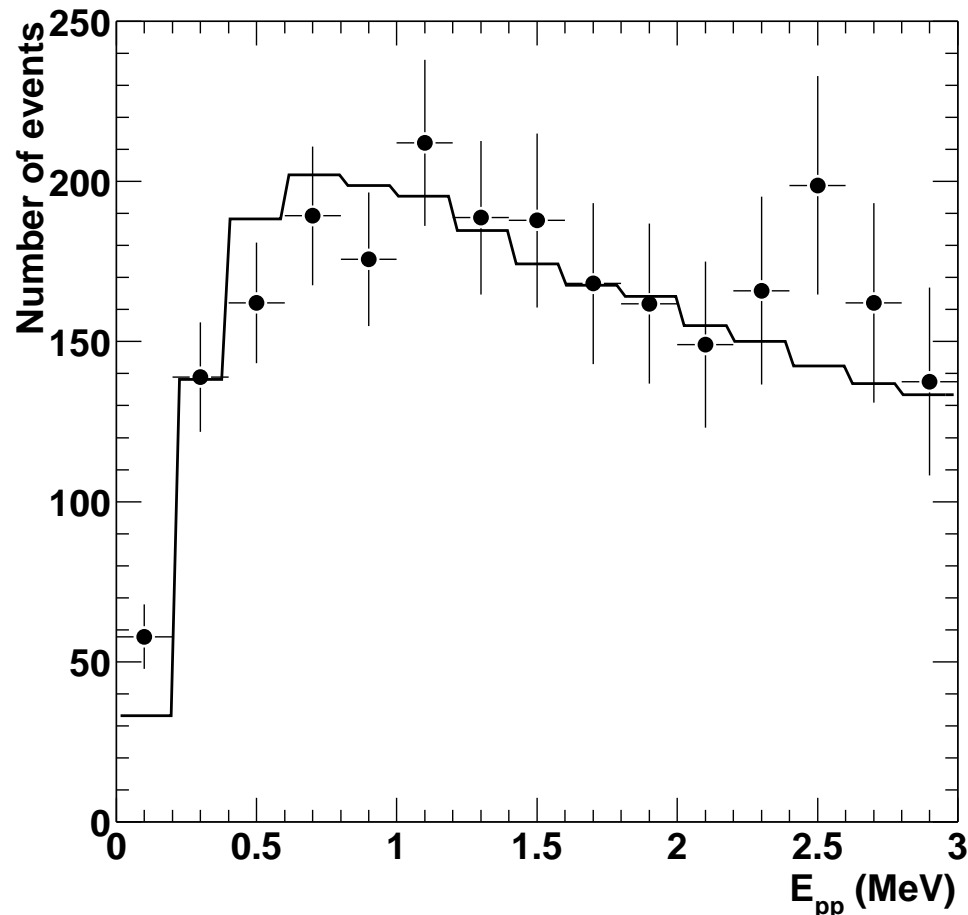


Fig. 5. Excitation energy distribution in comparison with the theoretical expectation (histogram) from fsi.

of the proton pair and its total momentum is nearly isotropic, but would allow a few percent of nonisotropic contamination to the differential cross section. The counting rates at high energies (1.35 and 1.9 GeV) were rather low. Therefore, in order to present the energy dependence of the process for all measured beam energies, the three-fold cross section was integrated over the

interval $0 < E_{pp} < 3$ MeV and averaged over the angular range $0 < \theta_{pp}^{\text{cm}} < 8^\circ$, resulting in

$$\overline{\left(\frac{d\sigma}{d\Omega_{pp}^{\text{cm}}}\right)} = \frac{N_{\text{cor}}}{L^{\text{int}} \cdot \Delta\Omega_{pp}^{\text{cm}}} \cdot \frac{N_{\text{sig}}}{N_{\text{sig}} + N_{\text{bg}}} \cdot f \quad (1)$$

(Table 1). Here $N_{\text{cor}} = \sum_{i=1}^N 1/(A_i \cdot \varepsilon_i)$, N is the number of selected proton pairs, A_i and ε_i correspond to acceptance and detector efficiency for registration of the i -th pair. The correction factor f , close to unity, accounts for several soft cuts applied during data processing. The acceptance was calculated as a function of E_{pp} and θ_{pp}^{cm} assuming a uniform distribution in ϕ_{pp}^{cm} and isotropy in the two proton system. The average detector efficiency was $\varepsilon \approx 90\%$.

The differential cross section obtained as a function of beam energy is shown in Fig. 6. The energy dependence of the measured cross section is similar to that of the $pd \rightarrow dp$ process, but its absolute value is smaller by about two orders of magnitude. There is no indication for the predicted dip in the breakup cross section. A comparison of the experimental results with the ONE+SS+ Δ calculations is shown also. At the lowest energies (0.6–0.7 GeV) the results for the Reid Soft Core (RSC) [31] and the Paris [32] potential reproduce rather well the measured breakup cross section. This energy range corresponds to the region where the $\Delta(1232)$ dominates in the $pd \rightarrow dp$ cross section. The theoretical curves for the breakup process exhibit a shoulder at ~ 0.5 GeV as well. This indicates that in spite of the isospin suppression, the contribution from the Δ is still important because of the nearby minimum of the ONE cross section. At higher energies, including the region of the expected dip at 0.7–0.8 GeV, the model is in strong disagreement with the data. One should note that the ONE+SS+ Δ model underestimates the $pd \rightarrow dp$ cross section

Table 1

Summary of the experimental results. T_p denotes the beam energy, L^{int} the integrated luminosity, N the number of events with $E_{pp} < 3$ MeV and pair emission angle $\theta_{pp}^{\text{cm}} < 8^\circ$, N_{cor} gives the number of events N , corrected for acceptance and detector efficiency, $N_{\text{sig}}/(N_{\text{sig}} + N_{\text{bg}})$ is the background correction, and $\overline{d\sigma/d\Omega_{pp}^{\text{cm}}}$ denotes the cross section (see Eq.(1)).

T_p [GeV]	L^{int} [$\text{cm}^{-2} \cdot 10^{34}$]	N	N_{cor}	$\frac{N_{\text{sig}}}{N_{\text{sig}}+N_{\text{bg}}}$	$\overline{d\sigma/d\Omega_{pp}^{\text{cm}}} \pm \sigma^{\text{stat}} \pm \sigma^{\text{syst}}$ [$\mu\text{b/sr}$]
0.6	1.41±0.12	339	1403	0.94 ± 0.05	1.72 ± 0.09 ± 0.17
0.7	1.93±0.17	227	872	0.87 ± 0.05	0.72 ± 0.05 ± 0.08
0.8	2.38±0.20	305	1050	0.89 ± 0.04	0.72 ± 0.04 ± 0.07
0.95	1.28±0.11	112	337	0.85 ± 0.07	0.41 ± 0.04 ± 0.05
1.35	0.69±0.06	16	45	0.79 ± 0.22	0.10 ± 0.02 ± 0.03
1.90	0.74±0.07	9	18	0.62 ± 0.27	0.03 ± 0.01 ± 0.01

in the dip region ($T_p \sim 0.8$ GeV) as well [33]. A possible explanation for this discrepancy is discussed in Ref. [4], where the contributions of NN^* components of the deuteron wave function are evaluated on the basis of a six quark model. Correspondingly for the breakup, effects from N^* exchanges and the contribution of the $\Delta\Delta$ component of the deuteron can possibly increase the cross section in this region and fill the dip. Other sizable contributions may arise from intermediate states of the pp pair at $E_{pp} > 3$ MeV, de-excited by rescattering on the neutron in the final state.

4 Conclusion

We report here the first measurement of the cross section of the $pd \rightarrow (pp)n$ reaction with a fast singlet pp pair emitted in forward direction at beam energies between 0.6 and 1.9 GeV. The measurement was carried out in collinear kinematics close to those of pd backward elastic scattering. The known mechanisms of the $pd \rightarrow dp$ process describe reasonably well the measured breakup cross section at low energies (0.6–0.7 GeV). At higher energies the calculations depend on the NN interaction potential at short distances and disagree with the data. Possible shortcomings of the model may be attributed at present to an inappropriate choice of the reaction dynamics or inadequate assumptions about the short-range structure of the deuteron. The latter could be remedied by more detailed calculations using modern NN potentials, which are in progress.

We would like to emphasize that a study of the $pd \rightarrow (pp)n$ reaction with detection of pp 1S_0 pairs provides a new tool to investigate the short-range NN interaction. For further insight, additional data, in particular polarization measurements, are needed to provide a complete set of observables. These experiments are foreseen at ANKE.

5 Acknowledgments

We are grateful to J. Haidenbauer (IKP, FZ Jülich) for providing the scattering wave functions for the Paris potential. Valuable discussions with C. Wilkin and his careful reading of the manuscript are appreciated. We would also like to acknowledge in particular the early contributions by O.W.B. Schult. Some of

us acknowledge the warm hospitality and support by FZ Jülich. This work was supported by the BMBF WTZ grants KAZ 99/001, RUS 00/211, and RUS 01/691, and by the Heisenberg–Landau program.

References

- [1] A.K. Kerman, L.S. Kisslinger, *Phys. Rev.* 180 (1969) 1483.
- [2] N.S. Craigie, C. Wilkin, *Nucl. Phys. B* 14 (1969) 477.
- [3] L.A. Kondratyuk, F.M. Lev, L.V. Shevchenko, *Phys. Lett. B* 100 (1981) 448.
- [4] Yu.N. Uzikov, *Phys. Part. Nucl.* 29 (1998) 583.
- [5] A. Boudard, M. Dillig, *Phys. Rev. C* 31 (1985) 302.
- [6] J. Arvieux et al., *Nucl. Phys. A* 431 (1984) 613.
- [7] L.S. Azhgirey et al., *Phys. Lett. B* 391 (1997) 22.
- [8] M. Tanifuji, S. Ischikava, Y. Iseri, *Phys. Rev. C* 57 (1998) 2493.
- [9] V.M. Kolybasov, N.Ya. Smorodinskaya, *Sov. J. Nucl. Phys.* 17 (1973) 630.
- [10] A. Nakamura, L. Satta, *Nucl. Phys. A* 445 (1985) 706.
- [11] O. Imambekov, Yu.N. Uzikov, L.V. Shevchenko, *Z. Phys. A* 332 (1989) 349.
- [12] O. Imambekov, Yu.N. Uzikov, *Sov. J. Nucl. Phys.* 47 (1988) 695.
- [13] O. Imambekov, Yu.N. Uzikov, *Sov. J. Nucl. Phys.* 52 (1990) 862.
- [14] A.V. Smirnov, Yu.N. Uzikov, *Phys. Atom. Nucl.* 61 (1998) 361.
- [15] Yu.N. Uzikov, *JETP Lett.* 75 (2002) 5.
- [16] Yu.N. Uzikov, *J. Phys. G: Nucl. Part. Phys.* 28 (2002) B13.

- [17] S. Barsov et al., Nucl. Instr. and Meth. A 462 (2001) 364.
- [18] R. Maier, Nucl. Instr. and Meth. A 390 (1997) 1.
- [19] A. Khoukaz et al., Eur. Phys. J. D 5 (1999) 275.
- [20] V. Franco, R.J. Glauber, Phys. Rev. 142 (1966) 1195.
- [21] E.T. Boschitz et al., Phys. Rev. C 6 (1972) 547.
- [22] O.G. Grebenjuk et al., Nucl. Phys. A 500 (1989) 637.
- [23] F. Irom et al., Phys. Rev. C 28 (1983) 2380.
- [24] G.W. Bennet et al., Phys. Rev. Lett. 19 (1967) 387.
- [25] N. Dalkhazhav et al., Sov. J. Nucl. Phys. 8 (1969) 196.
- [26] B.S. Aladashvili et al., J. Phys. G: Nucl. Part. Phys. 3 (1977) 7.
- [27] K.M. Watson, Phys. Rev. 88 (1952) 1163; A.B. Migdal, Sov. Phys. JETP 1 (1955) 2.
- [28] L. Dubal et al., Phys. Rev. D 9 (1974) 597.
- [29] A. Boudard, Thesis. CEA-N-2386, Saclay (1984).
- [30] P. Berthet et al., J. Phys. G: Nucl. Phys. 8 (1982) L111.
- [31] J.R.V. Reid, Ann. Phys. (NY) 50 (1968) 411.
- [32] M. Lacombe et al., Phys. Lett. B 101 (1981) 139.
- [33] According to Ref. [3] a coefficient of 0.8 in the ONE amplitude arising from the distortion of plane waves in the initial and final states is used to match the absolute value of the $pd \rightarrow dp$ cross section at $T_p < 0.3$ GeV.

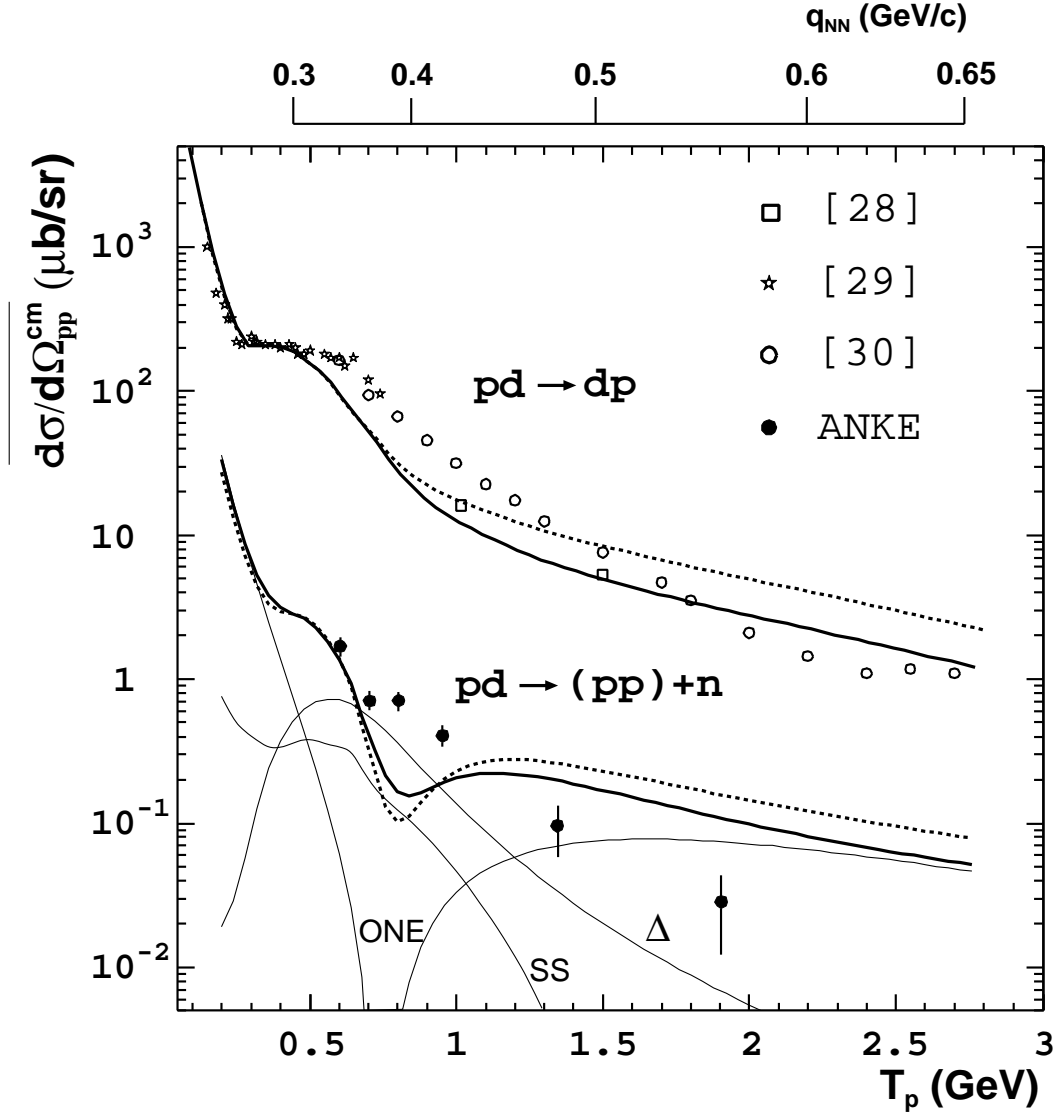


Fig. 6. Measured cross section of the process $pd \rightarrow (pp) + n$ for $E_{pp} < 3$ MeV versus proton-beam energy. The error bars include both statistical and systematic uncertainties (Table 1). Shown also are the $pd \rightarrow dp$ data ($d\sigma/d\Omega_p^{cm}$) taken from Refs. [28–30]. The calculations with the ONE+SS+ Δ model are performed using the NN potentials RSC (dotted line) and Paris (solid) [16] (note also Ref. [33]). The individual contributions of the ONE+SS+ Δ model with the Paris potential are shown by thin full lines. The upper scale indicates the internal momentum of the nucleons inside the deuteron for ONE in collinear kinematics at $E_{pp} = 3$ MeV.